OPTIMIZATION OF DESIGN PARAMETERS FOR A CONTACT SENSOR IN BUMPER-PEDESTRIAN IMPACT BY USING FE MODELS

AUTHORS:

Sunan HUANG[1], Dept. of Applied Mechanics, Chalmers University of Technology, Sweden
Jikuang YANG[1], Dept. of Applied Mechanics, Chalmers University of Technology, Sweden
Rikard FREDRIKSSON[2], Autoliv Research, Autoliv AB, Sweden

CORRESPONDENCE:

Sunan HUANG
Crash Safety Division, Department of Applied Mechanics, Chalmers University of Technology
SE 412 96 Gothenburg, Sweden
Telephone: +46 (0)703871420
Email: sunan.huang@chalmers.se

ABSTRACT

An active hood system was developed in Autoliv to minimize the head injury risk of pedestrians from impacts with car front. In order to detect the car-to-pedestrian impact in time, a contact sensor placed in the car bumper is needed. The stiffness of the bumper foam material is highly dependent on the environment temperature, which will result in unstable output from the contact sensor. A new pedestrian-bumper contact sensor was developed in Autoliv, in order to receive a stable output from the sensor at different temperatures.

In this study, the new contact sensor was analyzed and evaluated by using a bumper FE model of a production car. A baseline bumper FE model was firstly developed and validated by using EuroNCAP lower legform impact tests on the production car bumper. In order to improve the safety performance of the bumper FE model, the bumper foam material was softened and the foam thickness was increased. At the same time, the location, boundary condition and material property of the lower stiffener was also adjusted. As a result, the improved bumper model can meet the acceptance requirements of the EEVC WG17 lower legform impact test. A human lower extremity FE model was developed and the safety performance of the improved bumper was further evaluated by using the human lower extremity FE model. In the improved bumper model, the new

pedestrian-bumper contact sensor was integrated. A parameter study was conducted with two lower legform models in different masses and the diameter of the contact sensor tube was optimized in terms of the stability and mass sensitivity of the sensor output signals.

KEYWORDS:

Pedestrian Safety, Contact Sensor, Finite Element Simulation, Bumper Safety Performance

INTRODUCTION

Pedestrians are among the most vulnerable road user. In 2003, about 70,000 pedestrians were involved in motor vehicle collisions in the United States and 6.8% of them were killed. This percentage is 3.5 times higher than the average mortality of all the persons involved in motor vehicle collisions [1]. The pedestrian protection has become a research field which attracted much attention.

Different types of motor vehicles have been involved in the pedestrian accidents, but a number of statistical analyses on pedestrian accidents in motorized countries have indicated that passenger cars are overrepresented. In Europe, around 70% to 80% of the reported vehicles involved in the pedestrian accidents are passenger cars [2]. Some study has also shown that the hood of passenger cars is one of the main causes of fatal pedestrian injuries, including head-brain and thorax injuries [2].

In order to protect the pedestrian head and chest from serious impacts with the car bonnet, an active hood system, as shown in Figure 1, was developed in Autoliv. This system consists of a hood that is lifted in the rear end when a pedestrian is impacted by the car. Therefore, the distance between the hood and the hard inner parts of the car, such as the engine, becomes wider and a larger deformation of the hood in the pedestrian head and chest collision becomes possible. As a result, more impact energy can be absorbed and the injuries of the pedestrian are alleviated.

Figure 1 Active hood in activated (lifted) position [3]

One of the most important technical issues of the active hood system is how to identify the pedestrian crash on time. A contact sensor, which can be placed in the bumper, is therefore used as a solution. A potential problem of using the contact sensor was appeared: because of the unstable stiffness of the bumper foam, the output signal of the contact sensor changes with the varied environment temperature.

In order to stabilize the sensor output, a new sensor design was developed and tested in Autoliv Research Center. The main structure of the new sensor is a sealed air tube located in the bumper foam. When the environment temperature increases, the bumper foam around the tube will become softer but the air tube will become stiffer because of the higher air pressure in it. When the temperature decreases, the bumper foam will become stiffer but the air tube will become softer. By this way, the changing stiffness of the bumper foam will be compensated and the output signal of the sensor can keep stable.

The present study aims at analyzing and optimizing the new contact sensor. For this purpose, the baseline bumper FE model of a production car was developed and improved. Based on the improved bumper model, the new contact sensor was integrated and optimized.

MATERIAL AND METHOD

The baseline bumper FE model was firstly developed and validated by using the EuroNCAP lower legform impact tests on the production bumper. In order to improve the safety performance of the baseline bumper model, the bumper foam material was changed to softer 30g/l EPP foam and the foam thickness was increased. At the same, the position, boundary condition and material property of the lower stiffener were also

adjusted. Evaluated by the EEVC WG17 lower legform impact test, the improved bumper model can meet the acceptance requirements. A human lower extremity FE model was then developed based on the HUMOS2 full human body model. The safety performance of the improved bumper was further evaluated by the lower extremity model. In the improved bumper model, the new pedestrian-bumper contact sensor was integrated. A parameter study was conducted with two lower legform models in different masses and the diameter of the contact sensor tube was optimized in terms of the stability and mass sensitivity of the sensor output.

DEVELOPMENT AND VALIDATION OF THE BASELINE BUMPER FE MODEL

In Figure 2, the baseline bumper FE model of a production car (a large passenger car) is shown. This model consists of three basic parts: the bumper cover, lower stiffener and bumper foam. The pedestrian safety performance of the bumper is mainly decided by the material properties of these three parts and their boundary conditions.

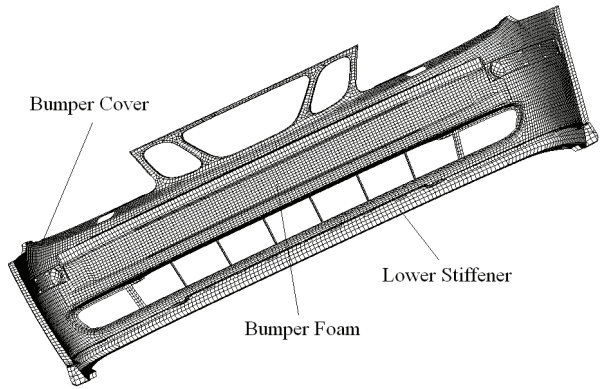

Figure 2 FE model of the production bumper

In 1998, the production car's EuroNCAP pedestrian impact tests were carried out at TNO Crash-Safety Research Center in Delft. The results from the lower legform impact tests on the bumper were listed in Table 1.

Table 1 Results of the production car's EuroNCAP lower legform impact tests

Test	Impact Location			Result		
	X (mm)	Y (mm)	Z (mm)	Tibia Acceleration (g)	Knee Bending (degree)	Knee Shearing (mm)
1	584	-478	499	158.5	31.8	4.06
2	508	-2	495	175.4	32.3	4.16
3	531	236	498	174.8	32.3	4.88

In order to evaluate the validity of the baseline bumper FE model, the EuroNCAP lower legform impact tests were simulated, as shown in Figure 3.

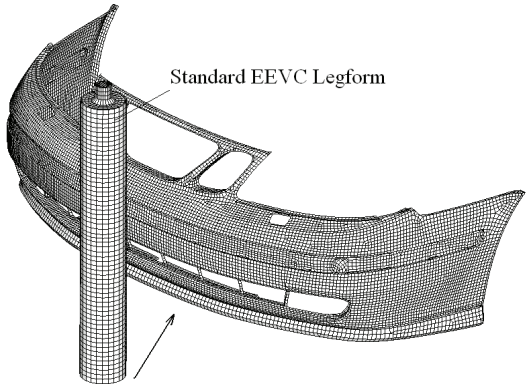

Figure 3 EuroNCAP lower legform impact simulation of the baseline bumper

Through the comparison of the results from the EuroNCAP tests and the corresponding simulations, the validity of the baseline bumper FE model was verified.

IMPROVEMENT OF THE BUMPER FE MODEL

According to the directive 2003/102/EC of the European Parliament and Council, from September 1st, 2010, the bumper system of any new production passenger car must meet the requirements of EEVC WG17 legform impact test. Otherwise, the member states of the European Union shall no longer grant EC type-approval or national type-

approval for this car [4]. From the lower legform impact tests and simulations of the baseline bumper, it was found that the tibia acceleration and knee bending angle could not meet the requirements of EEVC WG17. Therefore, the bumper design must be improved.

Development of the valid new bumper foam material model

The most important improvement of the bumper design is to change the bumper foam material from 80g/l foam to softer 30g/l EPP foam. For this change, the valid material model of the new bumper foam was developed.

As shown in Figure 4, the static compression strain-stress curves of the 30g/l EPP foam at -30, 23, 50 and 80°C were provided by the bumper foam manufacturer JSP. Based on the strain-stress curves, the new bumper foam material models at the temperature of -30, 20 and 85°C were developed.

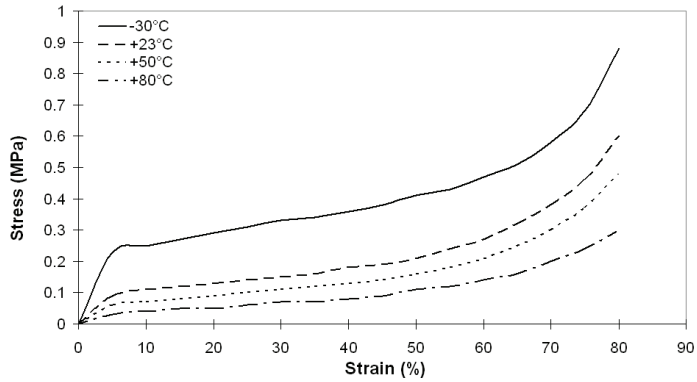

Figure 4 Strain-stress curves of 30g/l EPP foam

In Autoliv Research Center, simplified bumpers were used to test the new contact sensor. As shown in Figure 5, the cubic 30g/l EPP bumper foam was covered by the plastic bumper cover and fixed on a bracket. On the impact side of some bumpers, a ditch was cut out in the bumper foam to contain the sensor tube. A simplified legform impactor of 1.2 or 3Kg was used to impact the bumper. At the temperatures of -30, 20 and 85°C, 15 impacts were carried out. The legform accelerations were recorded and the air pressure changes in the tubes were output. It was found that at 20°C the stiffness of the bumper foam which was cut off for the ditch can be compensated by the sensor tube filled with 2.5bar air and the change of the initial air pressure in the tube can hardly influence the air pressure change during the impact.

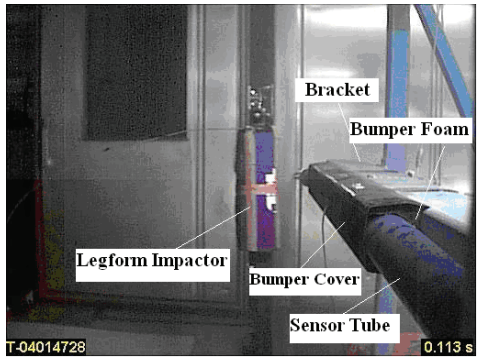

Figure 5 Autoliv impact test

In order to validate the material models of the 30g/l EPP foam, 11 successful tests were simulated, as shown in Figure 6.

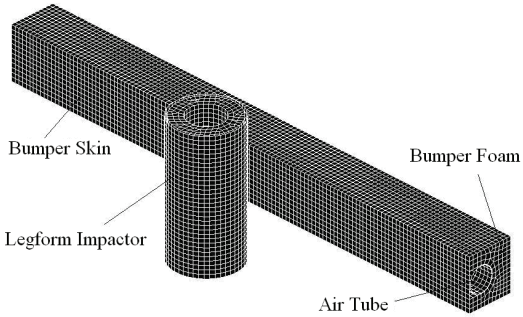

Figure 6 FE model of the Autoliv test

The legform acceleration curves from the Autoliv tests and corresponding simulations were compared. The similarity coefficients between the results from the tests and corresponding simulations were calculated by using Equation (1) and (2).

$$MagnitudeSimilarity = \frac{\int_{-\infty}^{\infty} x^2(t)dt}{\int_{-\infty}^{\infty} y^2(t)dt} \qquad \text{(Eq. 1)}$$

$$ShapeSimilarity = \frac{\int_{-\infty}^{\infty} x(t)y(t+h)dt}{\sqrt{\int_{-\infty}^{\infty} x^2(t)dt \int_{-\infty}^{\infty} y^2(t)dt}} \qquad \text{(Eq. 2)}$$

where

x(t) and y(t) is the legform acceleration from the impact test and corresponding simulation;

h is the phase difference between the two acceleration curves.

By using the calculated similarity coefficients, the validity of the new bumper foam material models was evaluated.

Improvement of the bumper FE model

In the improved bumper FE model, the bumper foam material was change from the 80g/l foam to the 30g/l EPP foam. Because the new bumper foam is much softer than the old, the thickness of the bumper foam was increased 30mm to ensure the enough deformation space.

From the validation of the baseline bumper FE model, it was found that because the lower stiffener is located too much behind the bumper foam, the legform model can hardly impact it. In the improved bumper model, the lower stiffener was therefore moved 50mm forward. 3 groups of linear springs (9 in each group) with the stiffness of 10N/mm were added to support it on the middle and right and left side. The Young's Modulus of the lower stiffener material was also increased 3 times. As a result, the impact force on the legform model can be scattered and the knee bending angle can be reduced. In Figure 7, the improved production bumper FE model is shown.

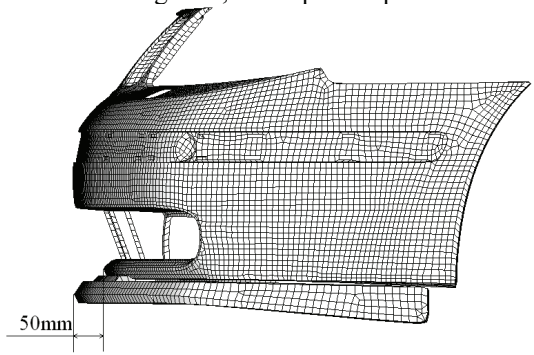

Figure 7 Improved bumper FE model

The safety performance of the improved bumper model was evaluated by the same impact configurations as the production car's EuroNCAP lower legform tests.

FURTHER EVALUATION OF THE IMPROVED BUMPER SAFETY PERFORMANCE BY THE HUMAN LOWER EXTREMITY MODEL

In order to verify the improved bumper safety performance for real pedestrian protection, a human lower extremity FE model was developed. The baseline bumper model and improve bumper model were impacted by the human lower extremity model. Through the comparison of the simulation results, the safety performance of the improved bumper was further evaluated.

Development and validation of the human lower extremity model

From the HUMOS2 full human body RADIOSS model, the right lower extremity was separated out and converted into LS_DYNA format, as shown in Figure 8. The materials of the bone, flesh and skin were kept same as the HUMOS2 model. According to the research of Nagasaka et al. (2004), the materials of the four major knee ligaments (ACL, PCL, MCL and LCL) were reset as an elasto-plastic model with strain rate-dependent characteristics and the material properties of the ligaments were also defined according to this research [5].

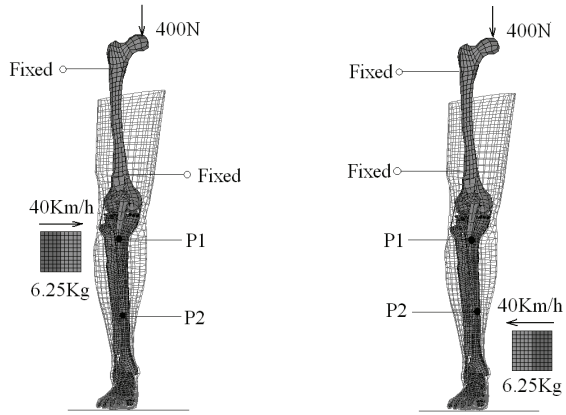

Figure 8 FE simulations of the knee shearing (left) and bending (right) tests

Kajzer et al. (1997) carried out 20 cadaver experiments to test the shearing and bending effects at the knee joint of the high speed lateral loading. In these experiments, each cadaver was lying supinely on a stable table. To simulate the weight of the upper body, a preload of 400N was applied on the tested lower extremity. A fixed foot plate was used to simulate the ground and provide a normal ground friction to the feet. The femur

was fixed at upper and lower positions. A styrodure covered impactor (6.25Kg) was used to impact the lower extremity under the knee joint for the shearing experiments and on the ankle area for the bending tests [6]. In order to validate the developed human lower extremity DYNA model, the experiment No. 16S (shearing experiment) and 7B (bending experiment) were simulated, as shown in Figure 8.

Further evaluation of the bumper performance

The baseline bumper model and improved bumper model was impacted by the validated human lower extremity FE model. As shown in Figure 9, only the bumper central line impacts were carried out and the impact speed was the same as EEVC lower legform test. From the simulations, the injuries of the lower extremity were observed and compared.

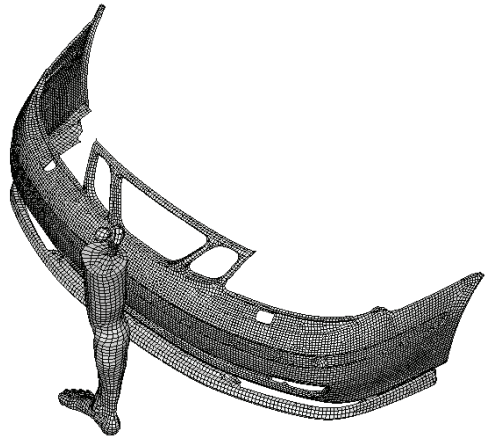

Figure 9 Impact between the human lower extremity and improved bumper

SENSOR OPTIMIZATION

Based on the improved bumper FE model, the sensor tube was introduced, as shown in Figure 10. The sensor tubes were simulated as a static airbag with two different diameters of 25mm and 50mm. At 20°C, the initial air pressure in the sensor tubes was 2.5bar and no leakage was considered.

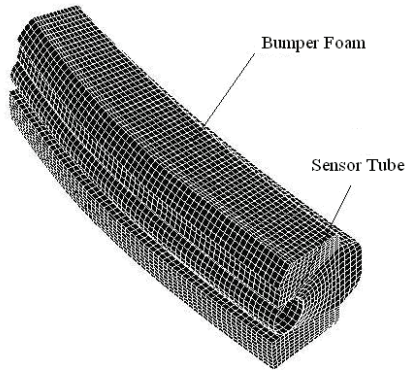

Figure 10 A half of the bumper foam model with the sensor tube

At 20°C, the safety performance of the improved bumper models with the sensor tubes was evaluated. It was found from the simulations that the models can still meet the EEVC WG17 lower legform impact requirements. The optimization of the sensor tube diameter was carried out based on the models.

This optimization aims at improving the stability and mass sensitivity of the new contact sensor's output. Because the output is the air pressure change in the sensor tube, the aim means that for the same impact object, the air pressure changes at different environment temperatures should keep as constant as possible; for the impact objects with different masses, the difference of the air pressure changes should be as large as possible.

The sensor tube was simulated as a static airbag. The air inside was regarded as ideal gas and no leakage was considered. The idea gas function can therefore be used to describe the change of the air state. In the optimization analysis, two different tube diameters were used and they are 25mm and 50mm. Through the comparison of the stability and mass sensitivity of the sensor output, the better diameter was decided. From the Autoliv tests, it was found that the change of initial air pressure in the sensor tube can hardly influence the air pressure change during the impact. The initial air pressures in these two kinds of air tubes at 20°C were thus set as 2.5bar to compensate the lost bumper stiffness of the cut-off bumper foam for the ditches. For the other two simulated environment temperatures of -30°C and 85°C, the initial air pressures in the tubes were calculated by the ideal gas function based on the constant volume assumption. At each temperature of -30°C, 20°C and 85 °C, the improved bumper models with the sensor tubes were impacted by both the EEVC WG17 standard legform model and 1 kg simplified legform model. As a result, the temperature stability and mass sensitivity of the sensor can be estimated.

RESULTS

VALIDATION OF THE BASELINE BUMPER FE MODEL

The results of the baseline bumper FE model validation were listed in Table 2.

Table 2 Simulation results for the baseline bumper model validation

No.	Impact Location			Result		
	X (mm)	Y (mm)	Z (mm)	Tibia Acceleration (g)	Knee Bending (degree)	Knee Shearing (mm)
1	584	-478	499	154.0	26.5	2.82
2	508	-2	495	192.0	31.5	3.87
3	531	236	498	207.0	31.0	3.72

From Table 2, it can be seen that the simulation results of the tibia acceleration and knee bending angle are comparable with the corresponding test results. The baseline bumper FE model is valid and can be used as the basis for further analysis.

DEVELOPMENT OF THE IMPROVED BUMPER FE MODEL

According to the strain-stress curves shown in Figure 4, the material model of the 30g/l EPP foam was developed at the temperature of -30, 20 and 85°C, as indicated in Table 3.

Table 3 Material model of the 30g/l EPP foam

Temperature	Material Model	Young's Module (MPa)	Strain-Stress Curve
-30°C	Low density foam	3.6	Compression curve at -30°C
20°C	Low density foam	1.8	Compression curve at 23°C
85°C	Low density foam	0.9	Compression curve at 80°C

In order to validate the material model of the 30g/l EPP bumper foam, the magnitude and shape similarity coefficients between the tibia acceleration curves from the impact tests and the corresponding simulations were calculated according to Equation (1) and (2) and listed in Table 4.

Table 4 Similarity coefficients between the tibia acceleration curves

Test	1	2	3	4	5	6	7	8	9	10	11
Magnitude	0.98	0.78	0.99	0.87	0.88	0.92	0.86	0.72	0.80	0.90	0.75
Shape	0.98	0.99	0.99	0.97	0.99	0.98	0.94	0.97	0.97	0.98	0.96

From Table 4, it can be seen that most of the similarity coefficients are close to 1. This means that the acceleration curves can coincide with each other well. The validity of the bumper foam material model was therefore verified.

Through the impact with the standard EEVC WG17 legform model, it was found that the improved bumper FE model can meet the requirements of EEVC WG17. The simulation results were listed in Table 5.

Table 5 Simulation results for the improved bumper model evaluation

No.	Impact Location			Result		
	X (mm)	Y (mm)	Z (mm)	Tibia Acceleration (g)	Knee Bending (degree)	Knee Shearing (mm)
1	584	-478	499	143.0	13.6	1.71
2	508	-2	495	149.0	9.9	2.38
3	531	236	498	151.0	12.6	1.54

FURTHER EVALUATION OF THE BUMPER PERFORMANCE BY THE HUMAN MODEL

Validation of the human lower extremity model

According to the research of Nagasaka et al. (2004) [5], the dynamic fidelity of the human lower extremity model was evaluated by the comparison of the impactor accelerations and P1 and P2 displacements on the impact direction. This comparison was shown in Figure 11 and 12.

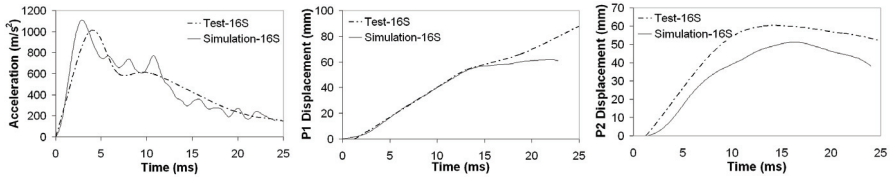

Figure 11 Comparison of the impactor acceleration and P1 and P2 displacement for the No. 16S test and simulation. Experiment results from Nagasaka et al. (2004) [5]

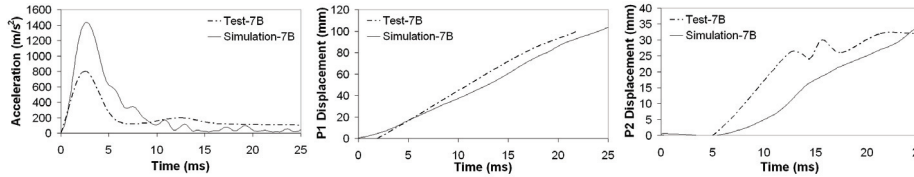

Figure 12 Comparison of the impactor acceleration and P1 and P2 displacement for the No. 7B test and simulation. Experiment results from Nagasaka et al. (2004) [5]

From Figure 11 and 12, it can be seen that except the impactor accelerations from the test and simulation 7B the dynamic responses of the human lower extremity model were comparable with the cadaver lower extremity.

The bio-fidelity of the model was validated by the comparison between the model predicted injuries and the actual injuries happened in the tests. As shown in Figure 13, in the simulation 16S, the anterior cruciate ligament (ACL) was avulsed and the tibia condyle was fractured. The avulsion of ACL was coincident with the only knee injury happened in the cadaver test 16S. The tibia condyle fracture was not observed in test 16S but it was a common injury type in the cadaver shearing tests. Therefore, this injury was considered as reasonable. From Figure 13, it can be see that the medial collateral ligament (MCL) and posterior cruciate ligament (PCL) were avulsed in the simulation 7B. Although these injuries were not observed in the test 7B, they were common in the cadaver bending tests and were acceptable here.

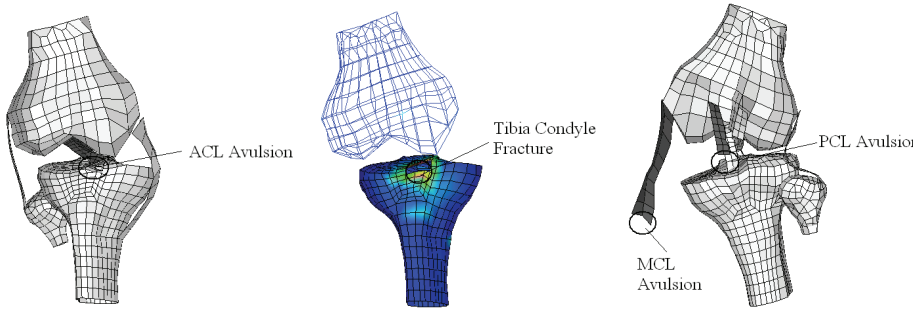

Figure 13 Knee injuries in the simulation 16S (left and middle) and 7B (right)

From the validation of the human lower extremity model, it can be seen that the dynamic responses of the model correlate well with the cadaver tests and the injuries predicted by this model are reasonable. Thus, this model is valid and can be used to evaluate the bumper models.

Further evaluation of the bumper performance

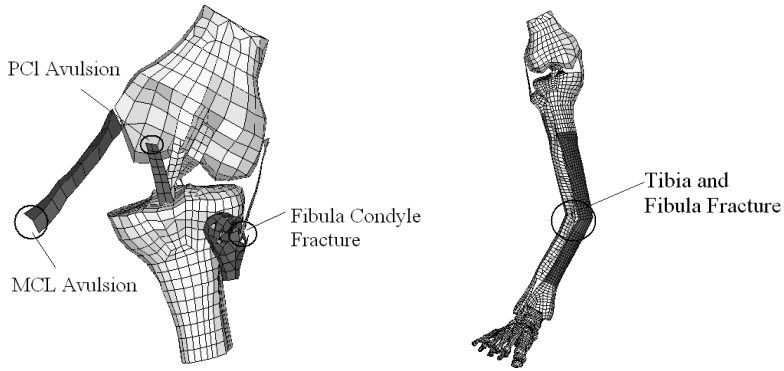

Figure 14 Lower extremity injuries from the impacts with the baseline (left) and improved (right) bumper

In Figure 14, the human lower extremity injuries from the impacts with the baseline and improved bumper model were shown. During the impact with the baseline model, the knee joint was largely bent. The medial collateral ligament (MCL) and posterior cruciate ligament (PCL) were avulsed. Because of the large impact force, the fibula condyle was also fractured. If impacted with the improved bumper model, the knee joint was much less bent and almost not injured. But because of the much stiffer lower stiffener used in this model, the tibia and fibula were fractured in the impact.

Through the comparison of the lower extremity injuries from these two simulations, it can be seen that the improved bumper model can better protect the knee joint during impact. But because of the stiffer lower stiffener, the risk of tibia and fibula fracture was increased. Considering the always higher cost and longer recover time of the knee joint injuries, the improved bumper can protect the human lower extremity better.

RESULTS OF THE OPTIMIZING ANALYSIS

The air pressure changes in the sensor tubes were obtained and processed by 100Hz filter, as shown in Figure 15 and 16.

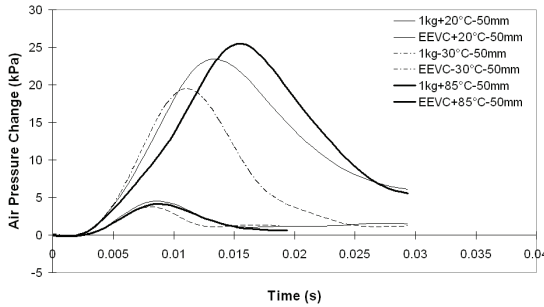

Figure 15 Air pressures changes in 50mm sensor tube

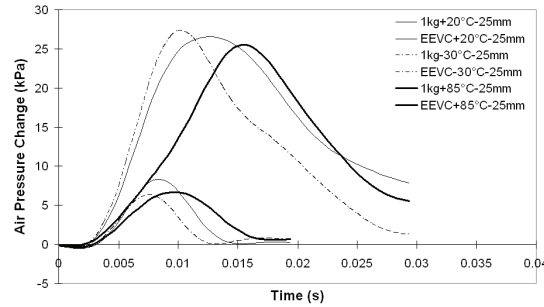

Figure 16 Air pressures changes in 25mm sensor tube

When 50mm sensor tube was used in the simulations, the peak values of air pressure changes in sensor tube can be classified into two groups obviously, as shown in Figure 15 and Table 6. The minimum distinction between these two groups of values is 14.9KPa. When 1kg legform impactor model was used in the simulations, the maximum difference of the air pressure change peak values is 0.8KPa and when the standard EEVC WG17 legform impactor model was used, the difference is 6KPa.

Table 6 Maximum air pressure change in 50mm sensor tube

Legform Impactor	Maximum Air Pressure Change (KPa)		
	-30°C	20°C	85°C
1kg legform	3.7	4.5	4.1
EEVC WG17 legform	19.4	23.4	25.4

If 25mm sensor tube was used, there are also two groups of air pressure change peak values, as shown in Figure 16 and Table 7. The minimum distinction between the two groups of values is 17.2KPa, a little larger than 14.9KPa from the simulations with 50mm sensor tube. When 1Kg legform impactor model was used, the maximum

difference of air pressure change peak values is 2KPa and when the standard EEVC WG17 legform impactor model was used, this difference is 1.8KPa.

Table 7 Maximum air pressure change in 25mm sensor tube

Legform Impactor	Maximum Air Pressure Change (KPa)		
	-30°C	20°C	85°C
1kg legform	6.3	8.3	6.7
EEVC WG17 legform	27.3	26.5	25.5

DISCUSSIONS

Air pressure change in sensor tube was analyzed in section 2. The idea gas function at constant temperature was used to describe the air in tube and no leakage has been considered. This function is also the mathematic basis of the simple air bag model which was used to simulate the sensor tubes. But in fact, this function can not describe the air in sensor tube perfectly. In this function, no dynamic character of air has been considered and it can only be used to describe the performance of static air. But the air in sensor tube is in fact high fluid during impact. This simplification of basic theory leads to a smaller and smoother air pressure change from simulation comparing with real test result. This difference is exampled in Figure 17. But by using this simplified theory, the correct tendency of air pressure change under different impact conditions can still be obtained.

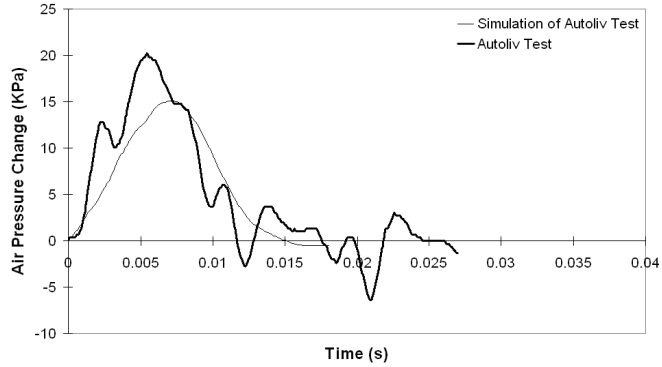

Figure 17 Air pressure changes from an Autoliv test and corresponding simulation

According to the idea gas function at constant temperature, if the compression ratio of air volume can keep constant, the increased initial air pressure in tube should also

increase the change of air pressure. But in the AUTOLIV test simulations, if we keep other factors constant, the increased initial air pressure has almost no obvious influence on the change of air pressure. The reason can be that the increase of initial air pressure in tube is equivalent to increasing the stiffness of the sensor tube. When the stiffness of the bumper foam around the sensor tube keeps constant, the sensor tube will become more difficult to compress. That means the compression ratio of air volume can not keep constant but will decrease. Therefore, only increasing the initial air pressure in tube is not a useful method to increase the change of air pressure during impact.

CONCLUSIONS

The baseline bumper model can not meet the acceptance requirements of the EEVC WG17 lower legform test. Through the improvement of the bumper design, the safety performance of the bumper model was improved and the results from virtual testing can meet the EEVC requirements for legform impact.

By using the human lower extremity FE model, the safety performance of the baseline and improved bumper model was further evaluated. It was found that by using the improved bumper model, the human knee joint can be much better protected but the risk of the tibia and fibula fracture was increased. Considering the comprehensive effect of the improved bumper design, a better lower extremity protection can be achieved.

The stability and mass sensitivity of the sensor output can be achieved by using two different diameters of the sensor tube. By using 25mm sensor tube, the sensor output can be more stable for the EEVC WG17 legform impact and more sensitive to the different masses of the impact objects. Therefore, the sensor tube with 25mm diameter is a better choice for the bumper contact sensor design.

REFERENCES

1. Federal Highway Administration: Pedestrian Safety Guide and Countermeasure Selection System, September 2004. Available from: http://www.walkinginfo.org/ [Accessed 25 Jan 2007]
2. Yang J.K., Otte D. and Yao J.F.: The Dynamic Responses and Head Injury Correlations of Child Pedestrians Involved in Vehicle Accidents, International Conference on Expert Symposium on Accident Research (ESAR), Hannover Germany, 3-4 September, 2004.
3. Fredriksson R., Haland Y. and Yang J.: Evaluation of a New Pedestrian Head Injury Protection System with a Sensor in the Bumper and Lifting of the Bonnet's Rear Edge, EVS Conference, 2001.

4. European Union: Directive 2003/102/EC of the European Parliament and of the Council, Official Journal of the European Union, 17 November, 2003.
5. Nagasaka K, Mizuno K, Tanaka E, Yamamoto S, Iwamoto M, Miki K and Kajzer J.: Finite Element Analysis of Knee Injury Risks in Car-to- Pedestrian Impacts, Traffic Injury Prevention, Vol. 4, No. 4, pp. 345-354, December, 2003.
6. Kajzer J., Schroeder G., Ishikawa H., Matsui Y., Bosch U., Shearing and Bending Effects at the Knee Joint at High Speed Lateral Loading, SAE Paper 973326, 1997.
7. European Enhanced Vehicle-safety Committee: Improved Test Methods to Evaluate Pedestrian Protection Affordable by Passenger Cars, EEVC Working Group 17 Report, December 1998 with September 2002 updates.
8. European New Car Assessment Programme (EuroNCAP): Pedestrian Testing Protocol, Version 4.1, March 2004.